IOPscience iopscience.iop.org

Home Search Collections Journals About Contact us My IOPscience

Probing the (001) surface of magnetite crystals by second harmonic generation

This article has been downloaded from IOPscience. Please scroll down to see the full text article.

2007 J. Phys.: Condens. Matter 19 396006

(http://iopscience.iop.org/0953-8984/19/39/396006)

View the table of contents for this issue, or go to the journal homepage for more

Download details:
IP Address: 129.252.86.83
The article was downloaded on 29/05/2010 at 06:08

Please note that terms and conditions apply.

IOP PUBLISHING JOURNAL OF PHYSICS: CONDENSED MATTER

J. Phys.: Condens. Matter **19** (2007) 396006 (10pp) doi:10.1088/0953-8984/19/39/396006

Probing the (001) surface of magnetite crystals by second harmonic generation

A A Rzhevsky[1,4], B B Krichevtsov[1], Y Su[2] and C M Schneider[3]

[1] Ioffe Physical Technical Institute, Russian Academy of Sciences, 194021 St Petersburg, Russia
[2] Institut für Festkörperforschung IFF-4, Forschungszentrum Jülich, 52425 Jülich, Germany
[3] Institut für Festkörperforschung IFF-9, Forschungszentrum Jülich, 52425 Jülich, Germany

Received 3 June 2007, in final form 6 August 2007
Published 3 September 2007
Online at stacks.iop.org/JPhysCM/19/396006

Abstract

The surface structural and magnetic properties of (100)-oriented Fe_3O_4 bulk crystals in the high-temperature phase (centrosymmetric, O_h) have been studied by nonlinear second harmonic generation (SHG). The analysis of the azimuthal and magnetic field dependences of the SHG signal at nearly normal light incidence shows that the surface crystalline and magnetic symmetry of the samples investigated cannot be described by a point symmetry group C_{4v}, contrary to what may be expected from the crystalline symmetry. Instead, the data are compatible with a symmetry of group m or even lower. The reasons for this discrepancy are attributed to an extreme sensitivity of the method to even small (∼1°–2°) misorientations from the (100) surface plane for this particular experimental geometry and to the presence of surface stresses induced by surface defects. In addition, we find that the magnetic contrast from Fe_3O_4(001) is rather large (∼60–80%) and contains a contribution to the magnetization-induced second harmonic generation (MSHG) signal, which depends quadratically on the surface magnetization.

1. Introduction

Magnetite—Fe_3O_4—is probably one of the oldest known ferromagnetic compounds, which in its high-temperature ($T > 125$ K) phase has a cubic centrosymmetric structure O_h. It experiences a renewed interest recently in the context of spintronics, as band structure calculations predicted a half-metallic character [1–3], which was to some extent confirmed by experiments [4]. As in spintronic devices, interfaces play a crucial role; the surface structure and surface magnetism of magnetite single crystals and thin films is an important issue, which is far from being completely understood up to now. The magnetic and transport properties in magnetite are sensitively influenced by the surface stoichiometry [5], crystal and surface

[4] Author to whom any correspondence should be addressed.

 © 2007 IOP Publishing Ltd Printed in the UK

structure [6, 7], the presence of magnetically modified layers [8], and peculiarities of the phase transformation during oxidation [9].

Up to now the surface structure and the magnetic properties of Fe_3O_4 crystals of different orientations have been studied by a variety of surface sensitive techniques, and in particular local probes such as atomic force microscopy (AFM), scanning tunneling microscopy (STM), and magnetic force microscopy (MFM). As mentioned above, however, the implementation of magnetic materials such as magnetite in spintronic devices creates heteromagnetic interfaces, which in most cases are crucial in determining the functionality of the device. In the study of these material systems it is therefore important to employ experimental techniques, which provide both surface and interfacial sensitivity, depending on the system under investigation. In fact, the method of optical second harmonic generation (SHG) is such an approach, as it is able to probe both surface as well as interface structural aspects. In its magnetically sensitive variant (magnetic SHG, MSHG) it is selectively probing the interface and surface magnetism in crystals and thin films. The interface sensitivity of SHG comes from the fact that a second harmonic generation signal involving electric dipole transitions is only allowed in non-centrosymmetric media, and at surfaces or interfaces of centrosymmetric media, where the inversion symmetry is broken. In magnetic crystals, along with the crystallographic (non-magnetic) contribution to SHG, a magnetic MSHG contribution induced by the magnetization, an external magnetic field or magnetic order parameter is also allowed. The non-magnetic SHG provides information about the electronic properties and crystal structure, while the magnetic SHG probes the magnetic properties of the material. MSHG has been proved to be a powerful optical tool and has been applied successfully to study the surface properties of magnetic crystals and thin films [10, 11].

In one of our previous experiments [14] we employed the MSHG approach to study the surface magnetic properties of Fe_3O_4/MgO(100) *thin films* (50 nm). In this system we observed that the azimuthal variation of the MSHG signal deviates significantly from the dependence expected from the C_{4v} point symmetry of an ideal (100)-oriented surface. In particular, we found a unidirectional component (with an angular periodicity of 360°) in the angular dependences of the MSHG signals $\Delta I(\phi)$ measured in ps and ss polarization combinations, which is forbidden for a strict C_{4v} symmetry. This behavior of the MSHG signal strongly suggests that the actual symmetry of the film surface (structural and/or magnetic) is lower than C_2. Among the possible mechanisms leading to such a symmetry lowering, a modification of the surface due to the coexistence of different oxide phases and a strong pinning of the magnetization at anti-phase boundaries were considered.

It should be noted that the crystal structure and magnetic properties of thin films and bulk crystals differ significantly, because of a large density of crystal twins and anti-phase boundaries in the film, resulting in an anomalous magnetic behavior [12, 13]. Also, in contrast to *bulk* magnetite, thin films reach magnetic saturation only in external fields much larger than the value of $H = 0.3$ T used in the above experiment [14]. These differences lead to an obvious question: How does the surface/interface magnetism in magnetite thin films and bulk crystals of the same orientation compare? Thus, the aim of this work is to study the surface crystal and magnetic structure of magnetite Fe_3O_4(100) single crystals by means of magnetization-induced second harmonic generation (MSHG). It should also be noted that second-order nonlinear optical susceptibilities giving rise to an SHG signal in magnetite bulk crystals have not yet been studied so far. In order to facilitate comparison with our thin-film results, a geometry of nearly normal light incidence has been chosen to investigate the bulk crystals. As we will show in the analysis for (100)-oriented samples, this experimental geometry provides the highest magnetic contrast and sensitivity to small changes in crystal structure.

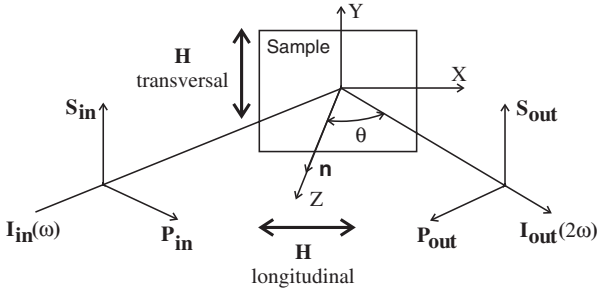

Figure 1. Geometry of the SHG measurements.

2. Experiment

In our studies we investigated three different magnetite $Fe_3O_4(100)$ single crystals grown by a floating zone method. They will henceforth be labeled N1 to N3. The diameter of the samples ranged between 5–10 mm and the thickness 1–3 mm. Our samples were polished with a 0.1 micrometer-sized diamond paste to obtain an optical quality of the surface. During the polishing process, the samples were constantly rotated to avoid any preferred orientation of possible scratches. The surface quality of all samples was further checked by measuring the rocking curve of the (400) Bragg reflection at different spots on the surface. A single and sharp rocking curve with a mosaic spread of less than 0.09° was obtained for all samples, indicating good crystal quality and the absence of any significant curvature, i.e. good flatness on the surface. X-ray analysis carried out on a Bruker D8 Advance diffractometer showed that global misorientation from the (100) plane is less than 2° in all samples. The crystal quality was judged by measuring the temperature characteristics of the conductivity. We observed a sharp Verwey transition exactly at 124 K, thus evidencing the high quality and ideal bulk stoichiometry of the crystals.

The nonlinear optical measurements were performed in a reflection geometry at nearly normal incidence of the light, $\theta \approx 5°$ (figure 1). The samples were mounted on a holder providing 360° azimuthal rotation around the surface normal (**z**). Azimuthal variations of the odd $\Delta I(2\omega) = I(+H) - I(-H)$ (MSHG) and even $I^{e}(2\omega) = (I(+H) + I(-H))/2$ contributions to the second harmonic generation (SHG) signal were recorded for different combinations of the polarization states of the incoming ($\hbar\omega_1 = 1.55$ eV) and outgoing ($\hbar\omega_2 = 3.1$ eV) light. The frequency of the fundamental beam lies in the relative transparency region of Fe_3O_4 (the absorption coefficient is $\sim 1 \times 10^5$ cm^{-1}), while the SHG frequency corresponds to a spectral region of the charge transfer ($Fe^{2+} \longrightarrow Fe^{3+}$) transitions [15–17]. The exciting light pulses with a duration of 200 fs were generated by a Ti:sapphire regenerative amplifier with a 1 kHz repetition rate. The pulses with an energy of 15 μJ were focused onto a spot of 0.5 mm diameter on the sample surface. The polarization of the fundamental and frequency-doubled light was chosen by appropriate orientation of the polarizer and analyzer, allowing one to investigate the SHG signal in four different polarization combinations (pp, ps, ss, sp). The fundamental light at $\lambda = 800$ nm was rejected by placing a blue filter (BG-39) into the reflected beam. The SHG signal was recorded using a photomultiplier and employing a photon counting technique. The counting time for each data point was usually 10–20 s. A magnetic field of up to 3 kOe was applied parallel to the sample surface either in the light incidence plane (longitudinal geometry, $\mathbf{H} \parallel \mathbf{x}$) or perpendicular to it (transversal geometry, $\mathbf{H} \parallel \mathbf{y}$). All measurements have been performed at room temperature (300 K) under ambient conditions.

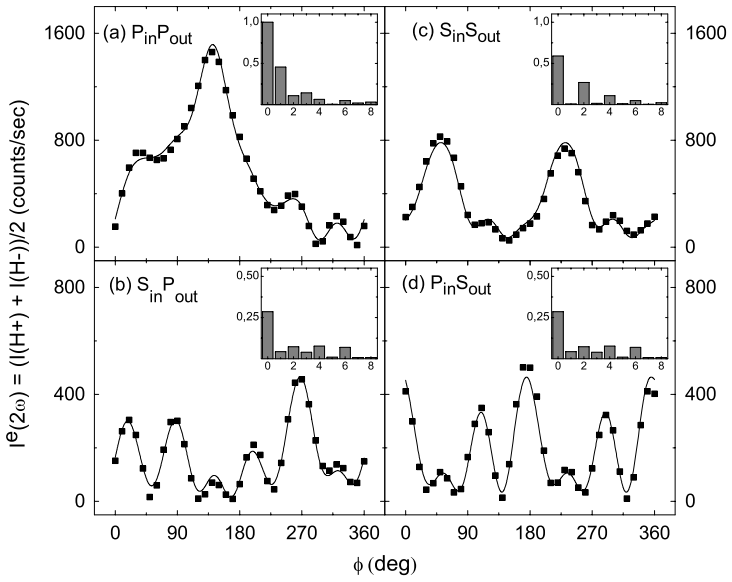

Figure 2. Azimuthal variations of the even on the external magnetic field H_{ext} contribution to the SHG signal for different polarization combinations of the ingoing (ω) and outgoing (2ω) light measured on sample N1. In the inset the relative amplitudes of the Fourier harmonics are shown (x means the harmonic order).

3. Results and discussion

From the nonlinear optical measurements, we extract two quantities, which behave even ($I^e(2\omega)$) and odd ($\Delta I(2\omega)$) with respect to the external magnetic field. The azimuthal variations of I^e and ΔI measured in longitudinal geometry for different combinations of input (ω) and output (2ω) polarizations of the light in the sample N1 are shown in figures 2 and 3. The respective azimuthal variations measured in the sample N2 are shown in figures 4 and 5. In the insets we show the relative amplitudes of different harmonics extracted from a Fourier analysis of the SHG azimuthal variations. It is apparent that the azimuthal variations measured on different crystals are quite complex and distinct, even for relevant combinations of light polarizations. We clearly see the presence of harmonics, which are odd and even in ϕ, where ϕ is the azimuth angle between the magnetic field **H** and the [100] direction of the film. It is important to note that, during these angular scans, the SHG and MSHG signals do not depend significantly on the position of the illuminated area of the sample surface. This clearly confirms that the observed variations of SHG reflect mainly the overall properties of the surface, but not the behavior of a singular point on the surface.

The following common features have been observed on all crystals. These are the appearance of remarkable zero-order as well as unidirectional (first-order angular harmonics with 360° periodicity) terms in I^e for the pp configuration (figures 2(a) and 4(a)). Another common feature is the biaxial contribution (fourth-order angular harmonics with 90° periodicity) in ΔI for pp polarization combination (figures 3(a) and 5(a)). Similarly, in ΔI for sp, ss, and ps polarization combinations the odd angular harmonics up to the seventh order dominate over the even ones, with the first-order angular harmonics being the largest in ss (figures 3(c) and 5(c)) and third-order in ps (figures 3(d) and 5(d)), correspondingly. For the sp polarization combination, different odd angular harmonics are approximately equally weighted

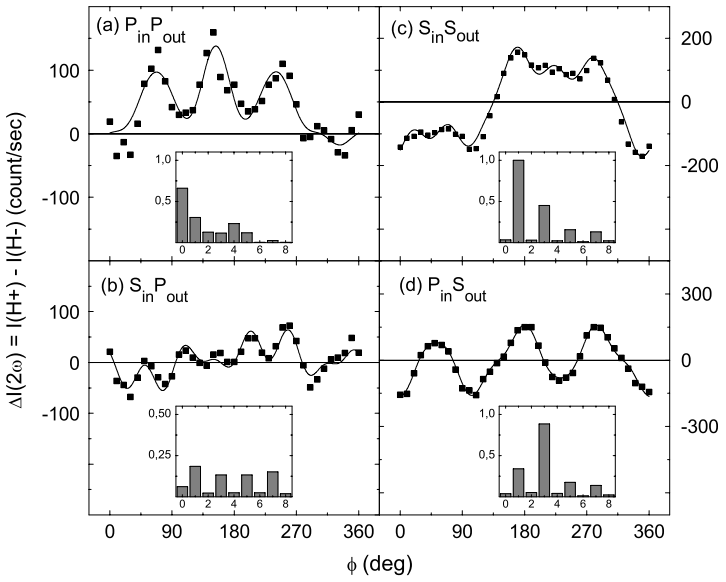

Figure 3. Azimuthal variations of the odd on H_{ext} contribution to the SHG signal for different polarization combinations of the incoming (ω) and outgoing (2ω) light in sample N1. In the inset the relative amplitudes of Fourier harmonics are shown (x denotes the harmonic order).

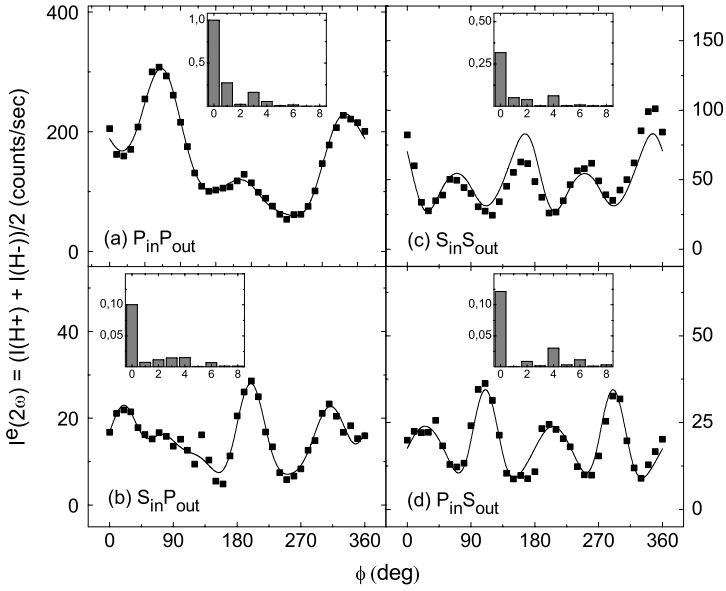

Figure 4. Azimuthal variations of the even on the external magnetic field contribution to the SHG signal for different polarization combinations of the incident (ω) and outgoing (2ω) light in sample N2. In the inset the relative amplitudes of the Fourier components are shown (x denotes the harmonic order).

(figures 3(b) and 5(b)). The most prominent distinction between these angular traces, however, is the occurrence of a first-order angular harmonic in I^e for the ss polarization combination in

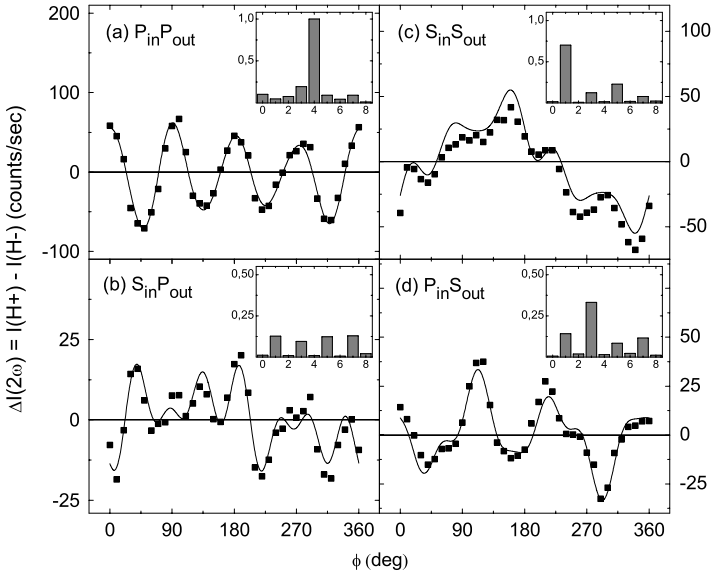

Figure 5. Azimuthal variations of the odd on the external magnetic field contribution to the SHG signal for different polarization combinations of the incident (ω) and outgoing (2ω) light in sample N2. In the inset the relative amplitudes of the Fourier components are shown (x denotes the harmonic order).

samples N2 (figure 4(c)) and N3 (not shown). This is apparently too small to be resolved for the sample N1. Besides, the presence of significant zero-order and first-order angular terms in ΔI (figure 3(a)) was observed in sample N1 for the pp polarization combination in contrast to the samples N2 and N3, where these are much smaller and the fourth-order angular term dominates. The magnitude of the magnetic contrast, defined as $\rho = \Delta I/2I^{e}$, is remarkably high and can reach 60–80% in the ps and ss polarization combinations.

Because Fe_3O_4 is a centrosymmetric system at $T = 294$ K, bulk-related electric-dipole contributions to the SHG signal are forbidden. Thus, mainly the broken symmetry at the surface and high-order mechanisms reflecting quadrupole or magnetic dipole symmetries may act as a source of a sizable SHG signal. In the analysis of the results we will neglect high-order mechanisms, assuming mainly an electric-dipole character of the SHG response.

A detailed analysis of the SHG characteristics measured on the (100) faces may be performed on the basis of a formalism developed in [19, 18]. For (100) surfaces described by a C_{4v} point symmetry, the crystallographic (non-magnetic) contribution to the SHG signal vanishes at exactly normal incidence ($\theta = 0$). Only even on **M** magnetic contributions to the second harmonic response ($\Delta I = 0$) are possible for all polarization combinations. This even contribution is anisotropic and can be described by a combination of the zeroth and eighth harmonics in ϕ. For the case of oblique incidence ($\theta \neq 0$), a non-magnetic contribution to the SHG arises in pp and sp polarizations, which is independent of the azimuth ϕ. It is forbidden, however, in ps and ss polarizations. Therefore, the odd magnetic contribution ΔI appearing in the pp and sp polarization combinations is a result of the interference of the non-magnetic and magnetic nonlinear optical susceptibilities. It can be described by a fourth harmonic in the ϕ signal.

Thus, from the quantities I^{e} and ΔI measured on the magnetite bulk crystals, as shown in figures 2–5, we see that the azimuthal variations differ distinctly from the expected behavior

of a surface layer described by a point symmetry C_{4v}. This is specifically indicated by the presence of odd harmonics in the angular dependence of I^e and ΔI. This finding points out that the real symmetry of the surface must be lower than C_{4v}. Furthermore, the existence of sizable odd angular harmonics in $I^e(\phi)$ allows us to exclude symmetry groups having even axes among the symmetry elements from our further consideration. As a consequence, the actual surface symmetry must be reduced to only monoclinic or triclinic point groups.

The azimuthal dependences of the SHG signals can be described using the following equation:

$$I^{kl}(2\omega) = I^e + \Delta I \sim |A^{kl}(\phi) + B_i^{kl}(\phi) \cdot M_i|^2$$
$$= |A^{kl}(\phi)|^2 + |(B_i^{kl}(\phi)M_i)|^2 + 2A^{kl}(\phi)B_i^{kl}(\phi) \cdot M_i \cos\delta_{AB}, \quad (1)$$

with $A^{kl}(\phi)$ and $B^{kl}(\phi)$ indicating the non-magnetic and magnetic susceptibilities, correspondingly. The indices kl relate to the different polarization combinations pp, ps, sp or ss, δ_{AB} is a phase shift, and $i = x, y, z$. The number of the nonlinear susceptibility tensor elements involved depends on the symmetry class considered. In [20] the SHG signal in anisotropic films of different symmetry classes has been analyzed and general expressions for $A^{kl}(\phi)$ and $B_i^{kl}(\phi)$, taking into account different polarization combinations, were deduced for the case of normal incidence.

We have fitted the azimuthal variations of I^e and ΔI measured in the different crystals using equations (11) and (15) of [20]. For this purpose we assumed a point symmetry m and included a constant term describing the small deviation from normal incidence ($\theta \approx 5°$) for pp and sp polarizations. The results of the fitting procedure are shown in figures 2–4 and 3–5 by the solid lines. A quite satisfactory description is achieved for the sample N1 if we assume the magnetic and non-magnetic nonlinear susceptibilities to both correspond to a monoclinic symmetry m. A characteristic feature of the results is the strong coupling of non-magnetic and magnetic SHG components. The fourth-order angular harmonic observed in ΔI for the pp situation (figure 3(a)) is caused by the interference of a non-magnetic constant term appearing due to a slight deviation from normal incidence and a magnetic term varying as a fourth harmonic in ϕ. The third-order harmonic in the azimuthal dependence of ΔI (figure 3(d)) arises due to the presence of third- and zero-order angular harmonics in non-magnetic and magnetic parts of the SHG, respectively. The appearance of the first-, fifth- and seventh-order angular harmonics for the sp polarization combination (figures 3(b) and 5(b)) is a result of the interference of first- as well as third-order non-magnetic and fourth-order magnetic angular harmonics in the corresponding nonlinear susceptibilities. The agreement between the experimental data and the calculated curves obtained for sample N1 confirms that the experimentally observed angular variations of SHG can indeed be described by a model of a surface layer with symmetry m.

At the same time, however, this model, assuming a *monoclinic* surface symmetry, leads to less satisfactory agreement for the samples N2 and N3. In these two cases the model clearly fails to describe the first angular harmonic contribution in I^e for the ss polarization combination (figure 4(c)). There is no *a priori* reason why the crystal N1 should differ that much from N2 and N3. Our finding therefore basically suggests that the number of independent coefficients in this symmetry class is insufficient and additional ones are required for a better description. A consistent description for all samples can be achieved, however, if we accept the symmetry of the surface to be eventually lower than monoclinic, i.e. to belong to the *triclinic* class.

Thus, the angular variations observed for both I^e and ΔI in all crystals investigated can be described by generally assuming a triclinic surface symmetry, which in some cases reduces to a monoclinic one. What are the physical mechanisms leading to these symmetry types? In general, a lowering of the surface symmetry may be caused by a small deviation of the

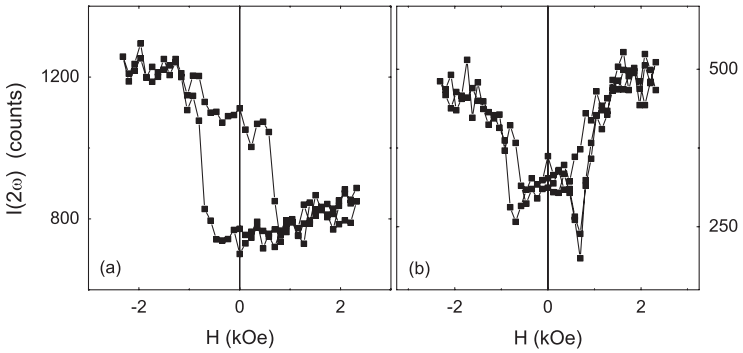

Figure 6. Magnetic field dependences of the SHG signal measured for the ss polarization combination at two different azimuthal angles in sample N2 when $A(\phi) \neq 0$ (a) and $A(\phi) \approx 0$ (b).

surface from the crystallographic (100) plane. The analysis of the SHG signal resulting from vicinal faces of cubic centrosymmetric crystals of Si with a misorientation of about 5° from the (100) plane showed that the non-magnetic part in the total SHG signal might be described by a set of angular harmonics up to eighth order [21, 22]. Since the non-magnetic susceptibility contributions at exactly normal incidence vanish in the case of a (100)-oriented surface, already a small misorientation from the (100) surface can lead to the appearance of a measurable SHG signal. The detection of this weak nonlinear signal is only a question of sufficient sensitivity of the experimental setup. If the surface normal does not coincide with the [001] crystallographic direction but is placed in one of the four symmetry planes, which are perpendicular to the (100) surface plane, the resulting surface symmetry will consequently reduce to the monoclinic class m. In all other cases, the symmetry should be triclinic. Note that the non-magnetic nonlinear susceptibilities may be very small, and their values might thus become comparable to the magnetic ones. The results of the calculations strongly suggest that this is the case for the samples investigated in our experiments.

In our previous experiments we found that in the Fe_3O_4 /MgO(100) thin films mainly zero- and fourth-order angular harmonics dominate in I^e for different polarization combinations, while fourth-order angular harmonics for pp and sp and first-order angular harmonics for ss and ps polarization combinations dominate in ΔI. In contrast to the results obtained for the films, both even and odd angular harmonics are present in I^e for the pp and sp polarization combinations in bulk crystals (see figures 2(a), (b) and 4(a), (b)). In the bulk samples, a third-order angular harmonic shows up in both I^e and ΔI. It is especially strong for the sp and ps polarization combinations in ΔI (see figures 3(b), (d) and 5(b), (d)). In thin films, the third-order angular term could not be resolved in I^e and is also much smaller in ΔI than in the bulk situation. Among the common features between bulk crystals and thin films we recognize the presence of a significant first-order angular harmonic in ΔI for ss and ps polarization combinations. This comparison shows that in bulk crystals the surface symmetry lowering manifests itself in a more pronounced way than in the epitaxial films. For example, the quantity ΔI, which is forbidden in C_{4v} symmetry, appears only in ss and ps polarization combinations, while in bulk crystals the forbidden ΔI and I^e appears practically in all polarization combinations.

In an alternative procedure, the information about the surface magnetization behavior can also be extracted from the magnetic field dependences of the SHG. The typical field variations of the SHG measured at different azimuths in sample N2 are compiled in figure 6. Because the parameters $A^{kl}(\phi)$ and $B^{kl}(\phi)$ in equation (1) may be of the same order of magnitude,

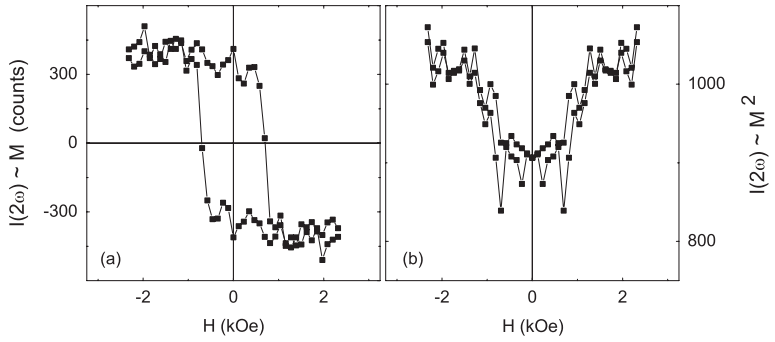

Figure 7. Linear (a) and quadratic (b) on magnetization parts of the SHG signal calculated from the field dependence presented in figure 6(a).

the dependence of $I(2\omega)$ on $\mathbf{M}$ can include both linear ($\sim 2A^{kl}(\phi)B^{kl}(\phi) \cdot M\cos\delta$) and quadratic ($\sim(B_i^{kl}(\phi)M_i)^2$) terms. If $A^{kl}(\phi) \neq 0$, the hysteresis loop of $I(2\omega)$ is defined by both contributions. In the case ($A^{kl}(\phi) = 0$) only the quadratic part of $I(2\omega)$ will be relevant. Both linear and quadratic on M_i contributions have been observed in the hysteresis loops for different orientations of the in-plane magnetic field in sample N2 corresponding to $A^{kl}(\phi) \neq 0$ (figure 6(a)) and $A^{kl}(\phi) \approx 0$ (figure 6(b)). For $A^{kl} \neq 0$, the separation of the linear and quadratic contributions may be performed by means of a symmetrization procedure, if we assume the magnetization hysteresis loop to be symmetric, $M_{\rightarrow}(+H) = -M_{\leftarrow}(-H)$, where $M_{\rightarrow}$ and $M_{\leftarrow}$ are the magnetization values corresponding to increasing and decreasing magnetic fields, correspondingly. The result of such a procedure is shown in figure 7. As one can see, the linear on M contribution displays a rectangular shape, reaching saturation at field strengths of approximately ± 1.0 kOe. This means that, in contrast to thin films, in the bulk crystals for the analysis of angle variations of the SHG in a field strength of $H = \pm 3$ kOe it is sufficient to account for the M_x component in the longitudinal geometry and for M_y in the transversal geometry. The azimuthal variation of the coercive field H_c is strongly anisotropic and shows a $C + D \times \sin(2\phi)$ behavior, with $(C + D)/(C - D) \approx 2$, where C and D are constant parameters. The anisotropy of H_c also independently indicates that the symmetry of the surface layer is lower than C_{4v}. The quadratic contribution extracted by means of this procedure ((figure 7(b))) is similar to the experimentally observed hysteresis loop at $A^{kl}(\phi) \approx 0$ (figure 6(b)).

In the above considerations, we proposed that the surface symmetry reduction may be caused by a small misorientation of the sample surface from the (100) plane. However, there may be other possible sources for such a surface symmetry reduction, which should not be excluded from the discussion. For example, the presence of other oxide phases such as maghemite (γ-Fe_2O_3) or hematite (α-Fe_2O_3) at the surface may effectively reduce the symmetry. In addition, the presence of surface stresses or a deformation due to a high density of surface defects or dislocations will also result in a symmetry lowering. In thin magnetite films prepared by molecular beam epitaxy (MBE) on well-oriented MgO substrates, the surface stresses should be much smaller than in a Fe_3O_4 bulk crystal. This may be one of the reasons why the MSHG response in films can be better described by a C_{4v} surface model than the respective bulk results. In order to completely exclude the possible presence of different oxide phases at the surface, future SHG experiments in high vacuum and carried out on properly prepared surfaces are needed. It would also be interesting to investigate the influence of the annealing temperature on the MSHG signal under conditions ($T > 300\,^{\circ}$C) where the formation of a hematite cap layer is observed [9].

4. Conclusions

The surfaces of several magnetite bulk crystals in the high-temperature (centrosymmetric) phase have been studied by magnetic-field-induced optical second harmonic generation. We found that the azimuthal variations of the SHG signal in near-normal incidence geometry are quite complex and cannot be simply described by a model of a surface with C_{4v} point group symmetry. The azimuthal characteristics of the non-magnetic and magnetic contributions to the SHG response can be satisfactorily described, however, if we assume a surface symmetry belonging to the monoclinic (or triclinic) class. The surface symmetry lowering may be related to a small misorientation ($\sim 2^\circ$) of the surface from the (100) crystallographic plane and the presence of surface stresses. The magnetic contrast is the largest for ss and ps polarization combinations and may reach values of 60–80% at different orientations of the in-plane magnetic field. The hysteresis loops of SHG at near-normal incidence involve contributions which are both linear and quadratic on magnetization. The linear contributions exhibit a rectangular shape with a considerable anisotropic character of the coercive field.

Acknowledgments

This work was supported by the Deutsche Forschungsgemeinschaft through SFB 491. We would like to thank V A M Brabers and R Claessen for providing samples of the bulk crystals. AAR and BBK gratefully acknowledge financial support through the Russian Foundation of Basic Research (grant no. 05-02-16451-a).

References

[1] Yanase A and Siratori K 1984 *J. Phys. Soc. Japan* **53** 312
[2] de Groot R A and Buschow K H J 1986 *J. Magn. Magn. Mater.* **54–57** 1377
[3] Zhang Z and Satpathy S 1991 *Phys. Rev.* B **44** 13319
[4] Dedkov Yu S, Rüdiger U and Güntherodt G 2002 *Phys. Rev.* B **65** 064417
[5] Fontijn W F J, van der Heijden P A A, Voogt F C, Hibma T and van der Zaag P J 1997 *J. Magn. Magn. Mater.* **165** 401
[6] Mariotto G, Murrphy S and Shvets I V 2002 *Phys. Rev.* B **66** 245426
[7] Stanka B, Hebenstreit W, Diebold U and Chambers S A 2000 *Surf. Sci.* **448** 49
[8] Parkin S S P, Sigsbee R, Felici R and Felcher G B 1986 *Appl. Phys. Lett.* **48** 604
[9] Zhou Y, Jin X, Mukovskii Y M and Shvets I V 2004 *J. Phys.: Condens. Matter* **16** 1
[10] Fiebig M, Pavlov V V and Pisarev R 2005 *J. Opt. Soc. Am.* B **22** 96
[11] Kirilyuk A and Rasing Th 2005 *J. Opt. Soc. Am.* B **22** 148
[12] Margulies D T, Parker F T, Rudee M L, Spada F E, Chapman J N, Aitchison P R and Berkowitz A E 1997 *Phys. Rev. Lett.* **79** 5162
[13] Margulies D T, Parker F T, Spada F E, Goldman R S, Li J, Sinclair R and Berkowitz A E 1996 *Phys. Rev.* B **53** 9175
[14] Rzhevsky A A, Krichevtsov B B, Rata A D, Chang C F, Sutarto R, Tjeng L H and Schneider C M 2006 *J. Appl. Phys.* **99** 08J702
[15] Schlegel A, Alvarado S F and Wachter P 1979 *J. Phys. C: Solid State Phys.* **12** 1157
[16] Fontijn W F J, Van der Zaag P J, Devillers M A C, Brabers V A M and Metselaar R 1997 *Phys. Rev.* B **56** 5432
[17] Park S K, Ishikawa T and Tokura Y 1998 *Phys. Rev.* B **58** 3717
[18] Atkinson R and Kubrakov N F 2001 *Phys. Rev.* B **65** 014432
[19] Hübner H and Bennemann K H 1995 *Phys. Rev.* B **52** 13411
[20] Gridnev V N, Pavlov V V, Pisarev R V, Kirilyuk A and Rasing Th 2001 *Phys. Rev.* B **63** 184407
[21] Bottomley D J, Lüpke G, Meyer C and Makita Y 1995 *Opt. Lett.* **20** 453
[22] Lüpke G, Bottomley D J and van Driel H M 1994 *J. Opt. Soc. Am.* B **11** 33